OPTIMIZATION OF HOT WORKABILITY AND HOT DEFORMATION MECHANISMS IN FeAl AND Fe_3Al BASED ALLOYS

Y.V.R.K.Prasad*, D.H.Sastry*, R.S.Sundar and S.C.Deevi

Chrysalis Technologies Incorporated, Richmond, VA 23237, USA
*Department of Metallurgy, Indian Institute of Science, Bangalore 560012, India

Abstract

The constitutive flow behaviors of powder extruded Fe-24 wt.%Al alloys prepared from gas atomized and water atomized powders have been examined in the hot working range using isothermal compression tests in a wide strain rate range with a view to optimize their hot workability and evaluate the mechanisms of hot deformation. The stress-strain curves for both these materials exhibited flow softening at strain rates above 1 s^{-1} while steady-state behavior was observed at lower strain rates. Using the standard kinetic rate equation to relate the flow stress with temperature and strain rate, an apparent activation energy of 430-465 kJ/mole has been evaluated and this value is much higher than that for diffusion of Fe or Al in FeAl. On the basis of the strain rate sensitivity of flow stress as a function of temperature and strain rate, processing maps have been developed, interpreted and confirmed microstructurally. The processing map for the gas-atomized iron aluminide exhibited dynamic recrystallization (DRX) in a wide temperature and strain rate window with an optimum occurring at 1075°C and 0.1 s^{-1}. On the other hand, the water atomized iron aluminide alloy dynamically recrystallized in the initial stages of deformation resulting in a stable fine grained structure which at larger strains caused superplastic deformation at strain rates lower than 0.1 s^{-1} and DRX at strain rates higher than 10 s^{-1}. The difference in the behavior is attributed to the presence of fine oxide and carbide particles in the water atomized aluminide. The gas atomized material is more prone to flow localization at higher strain rates than the water atomized alloy. Processing maps have also been developed on binary Fe_3Al and ternary Fe_3Al-X (X=Cr,Mn) in the temperature range 750-1050°C and strain rate range 0.001 – 10 s^{-1}. The map for the binary alloy exhibited a DRX domain in the temperature range 850 – 1050°C with its peak efficiency occurring at 1050°C at 0.01 s^{-1}. An apparent activation energy of 260 kJ/mole has been estimated for this mechanism and this value is close to that for diffusion of Al in Fe_3Al. Addition of Cr to this alloy did not significantly affect the general hot working features, although the DRX domain has moved to lower strain rates. However, the addition of Mn has strengthened Fe_3Al, suppressed DRX and promoted large grained superplasticity. Both these alloying additions have increased the apparent activation energy for hot deformation to about 350 kJ/mole. Optimum hot working of the Fe_3Al alloys requires in general slower strain rates and lower temperatures than the FeAl alloys.

Structural Intermetallics 2001
Edited by K.J. Hemker, D.M. Dimiduk, H. Clemens,
R. Darolia, H. Inui, J.M. Larsen, V.K. Sikka,
M. Thomas and J.D. Whittenberger
TMS (The Minerals, Metals & Materials Society), 2001

Introduction

Iron-aluminum system exhibits the formation of several intermetallic compounds out of which FeAl and Fe_3Al based alloys are being exploited for commercial applications as high temperature materials [1,2]. At ambient temperatures, FeAl has a B2 type ordered structure while Fe_3Al has a DO_3 type structure and both these are BCC derivatives. For obtaining the required high temperature ductility and strength as well as corrosion resistance to compete with other high temperature materials, it has been found necessary to alloy the compounds with elements like Cr, Mn, Zr or Mo. Another aspect of importance is the processing of these intermetallic alloys and in this direction several melting techniques [3,4] as well as powder metallurgy routes have been explored [5]. While roll compaction and sintering methods have been standardized for the manufacture of FeAl alloy sheets, hot extrusion of P/M billets is considered to be an important step for achieving dynamic mechanical properties like fracture toughness and impact resistance.

Lin and coworkers [6,7] have shown that FeAl alloys exhibit superplasticity which may be explored for component manufacture in conjunction with diffusion bonding. For designing the deformation processing route and optimizing the hot workability, it is essential to characterize the constitutive flow behavior of the intermetallic alloys in a range of deformation conditions and also evaluate the mechanism of hot deformation so that microstructural control may be achieved. Furthermore, it is well known that the intrinsic workability is sensitive to the chemistry, the initial microstructure and the prior processing history of the material. The aim of the investigation is to characterize the constitutive behavior in correlation with these aspects of the material.

Different approaches available for optimizing the hot workability and evaluating the hot working mechanisms have been reviewed in detail [8] and these include examination of shapes of stress-strain curves, evaluating kinetic parameters and developing processing maps. Although flow softening or oscillations in the stress-strain curves are indications of dynamic recrystallization (DRX), they are not considered to be conclusive evidences. The kinetic parameters are evaluated on the basis of the kinetic rate equation representing the relationship between the steady state flow stress (σ), strain rate ($\dot{\varepsilon}$), and the temperature (T) given by [9]:

$$\dot{\varepsilon} = A\sigma^n \exp[-Q/RT] \qquad (1)$$

where n is the stress exponent (inverse of strain rate sensitivity, *m*, of flow stress), Q is the activation energy, and R is the gas constant. The kinetic parameters, n and Q may be evaluated from the experimental data and compared with known values of some atomistic mechanisms like diffusion. However, this approach has the limitations that the value of apparent activation energy in alloys is often too complex to be attributed to a single atomistic mechanism and that it does not help in optimizing hot workability. In recent years, the technique of processing map is found to be useful for optimizing hot workability and controlling microstructure during hot working. The basis and principles of this approach are described earlier [10] and its validation on a wide variety of materials is demonstrated in a recent compilation [11]. In brief, the processing map consists of the superimposition of a power dissipation map and an instability map. The former map represents the manner in which energy is dissipated by the material through microstructural changes, the rate of which is represented by a dimensionless parameter called efficiency of power dissipation (η) in comparison with an ideal linear dissipator:

$$\eta = \frac{2m}{m+1} \qquad (2)$$

The instability map consists of the continuum instability criterion developed on the basis of the extremum principles of irreversible thermodynamics as applied to large plastic flow [11] represented by another dimensionless parameter given by:

$$\xi(\dot{\varepsilon}) = \frac{\partial \ln[m/(m+1)]}{\partial \ln \dot{\varepsilon}} + m \leq 0 \qquad (3)$$

The processing map exhibits domain with local efficiency maxima representing specific microstructural mechanisms as well as regimes of flow instabilities.

Experimental

The FeAl alloy specimens were produced by hot extrusion of gas atomized or water atomized powders sealed in a steel can. The chemical composition (in wt.%) of the billets is given in Table 1. It may be noted that the oxygen content in the water atomized powder is substantially higher. The hot extruded billets were fully dense and the microstructure consisted of dynamically recrystallized grains along with fine carbide and alumina particles aligned in the extrusion direction. The average grain diameter measured on the initial billets is given in Table 1.

The Fe_3Al alloys were prepared using vacuum induction melting and were tested in as-cast and homogenized condition. The chemical compositions in wt.% are given in Table 1. The initial microstructure of these material exhibited coarse equiaxed grains and the average grain diameters are given by Table 1.

Hot compression tests were conducted on cylindrical specimens of 10 mm diameter and 15 mm height and details of the experimental procedure was described in an earlier paper [13]. FeAl alloys were tested in the temperature range 750 – 1150°C and strain rate range 0.001 – 100 s^{-1} while Fe_3Al alloys were tested in the range 750 – 1050°C and strain rate range 0.001 – 10 s^{-1}. All the specimens were soaked for about 15 min, deformed to half their height and air cooled to room temperature after deformation. The deformed specimens were sectioned parallel to the compression axis and the cut surfaces were prepared for metallographic examination using standard techniques.

The load – stroke data obtained in compression were processed to obtain true stress –true plastic strain curves using the standard equations. The flow stress data obtained at different temperatures, strain rates and strains were corrected for adiabatic temperature rise, if any, by linear interpolation between log σ and 1/T. A cubic spline fit between log σ and log $\dot{\varepsilon}$ was used to obtain the strain rate sensitivity of flow stress as a function of

TABLE 1. Chemical composition in wt.% of the iron aluminide alloys and the average grain diameter in the starting billets used in the investigation

Element →	Al	Mo	Zr	B	C	O	Cr	Mn	Fe	Avg.Grain Dia., μm
Gas Atomized FeAl	24.0	0.42	0.1	0.005	0.06	0.05	-	-	Bal.	13
Water Atomized FeAl	24.0	0.42	0.1	0.005	0.06	0.31	-	-	Bal.	22
Fe_3Al	15.5	-	-	-	-	-	-	-	Bal.	520
Fe_3Al-Cr	16.3	-	-	-	-	-	2.7	-	Bal.	680
Fe_3Al-Mn	16.9	-	-	-	-	-	-	3.1	Bal.	740

strain rate. This was repeated at different temperatures. The efficiency of power dissipation through microstructural changes was then calculated as a function of temperature and strain rate using Eq.(2) and plotted as an iso-efficiency contour map. The data were also used to evaluate the flow instability parameter $\xi(\dot{\varepsilon})$ using Eq.(3) as a function of temperature and strain rate to obtain an instability map. These two maps were superimposed to obtain a processing map.

Results and Discussion

(i) FeAl Alloys

The true stress – true plastic strain curves obtained on gas atomized FeAl alloys at deformation temperatures of 900 and 1100°C and at different strain rates are shown in Fig.1 (a) and (b), respectively. The curves for the water atomized FeAl at 900°C and 1150°C are shown in Fig.2 (a) and (b).

At all the temperatures, the gas atomized FeAl alloy is harder than the water atomized alloy as may be expected from its finer grain size. At strain rates lower than about 1.0 s^{-1}, the flow curves for both the materials are essentially of steady-state type. However, at higher strain rates, the flow curves exhibited flow softening, which ended up in a steady state at 10 s^{-1} only in the case of water atomized alloy. Further, at higher temperatures (Fig.1b and Fig.2b), and at a strain rate of 1.0 s^{-1}, both the materials exhibited oscillations in the initial stages of deformation, which are however damped at higher strains.

It is not possible to predict the mechanisms of hot deformation from the stress-strain behavior alone since different mechanisms lead to similar behavior, e.g. DRX or unstable flow may lead to flow softening or oscillations. However, the temperature and strain rate dependence of flow stress may be analyzed further using other models.

Using the kinetic rate equation (Eq. 1), the activation parameters are evaluated assuming that the stress exponent is independent of strain rate. The apparent activation energy for hot deformation is estimated to be about 465 kJ/mole for gas atomized FeAl while it is slightly lower (about 430 kJ/mole) for the water atomized material. These values are in good agreement with those reported by other investigators [14-17] but are much higher than the activation energy for diffusion of either Fe or Al in FeAl compound [18, 19]. In view of this discrepancy, it is necessary

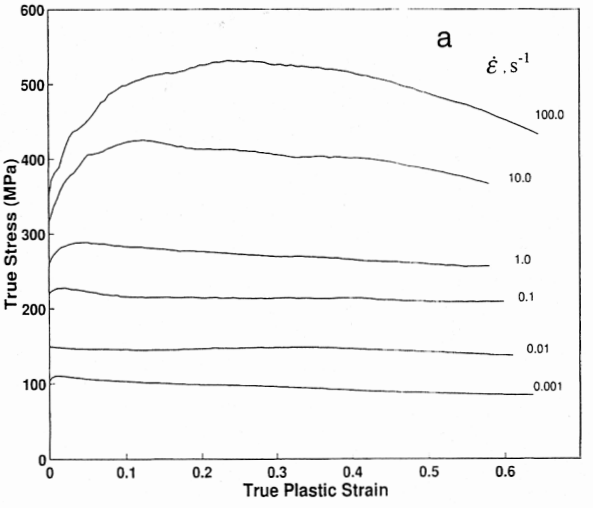

Fig. 1 True stress – true plastic strain curves for gas atomized FeAl material at different strain rates (a) at 900°C (b) at 1100°C.

to apply the other model viz., processing maps, to evaluate the hot deformation mechanisms described further below. Referring to Fig.3, the map for gas atomized material exhibits a single to

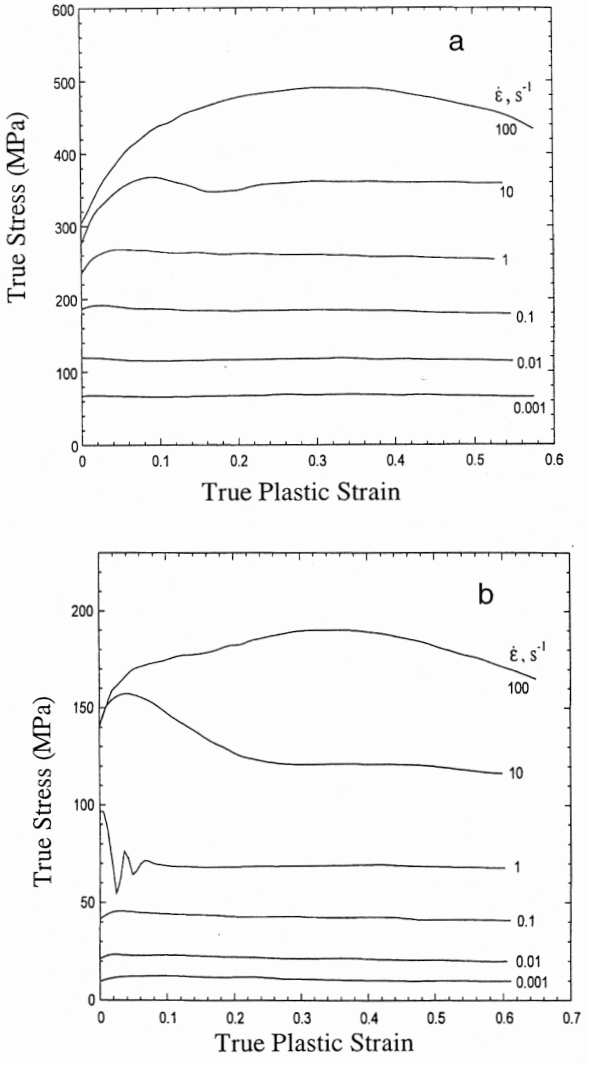

Fig. 2 True stress – true plastic strain curves for water atomized FeAl material at different strain rates (a) at 900°C (b) at 1150°C.

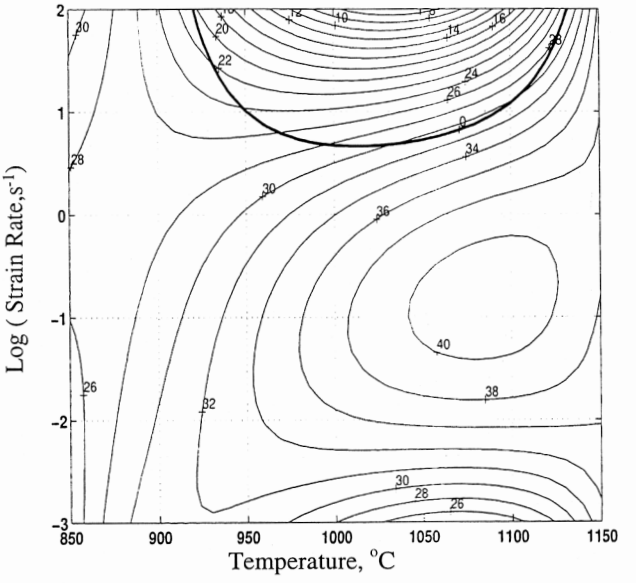

Fig. 3 Processing map for gas atomized FeAl at a strain of 0.4. The numbers against the contours indicate efficiency expressed in per cent. The regime over the dark line represents flow instability.

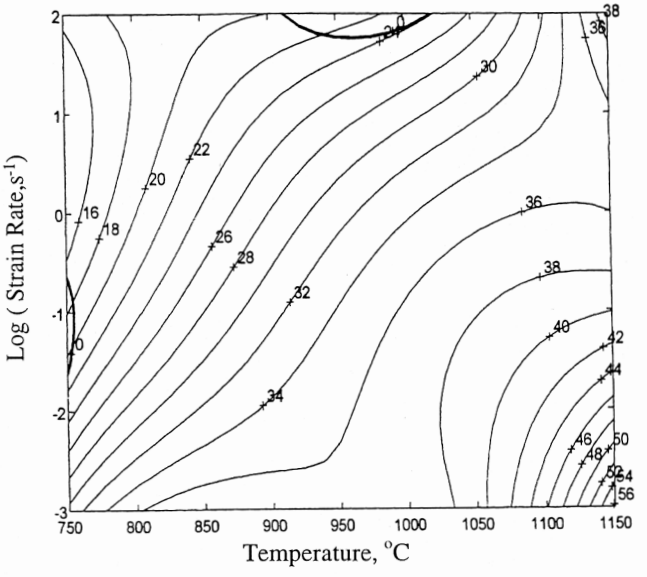

Fig. 4 Processing map for water atomized FeAl at a strain of 0.3. The numbers against the contours indicate efficiency expressed in per cent. The regime over the dark line represents flow instability.

with a peak efficiency. Detailed analysis of the microstructural development, the influence of temperature and strain rate on the grain size of deformed specimens has confirmed [20] that the domain represents DRX, which is a coveted mechanism for optimizing hot workability and reconstituting the microstructure. It may be noted that the DRX domain extends from 950°C to 1150°C and a strain rate range of 0.01 – 3 s^{-1}. Since the workability peak matches with that for the efficiency in the domain, the optimum hot workability occurs at 1075°C/0.1 s^{-1}. As regards the grain size relationship with the processing parameters, finer grain sizes result at lower temperatures (<1050°C) and higher strain rates (>0.1 s^{-1}).

Referring to the processing map for water atomized FeAl alloy (Fig.4), it exhibits two domains – one at strain rates below about 0.1 s^{-1} and temperatures above 1000°C with a peak efficiency of about 56% and the second at strain rates higher than 10 s^{-1} and temperature of 1150°C with a lower peak efficiency of 38%. On the basis of detailed microstructural examination and ductility correlations [13], the former domain is interpreted to represent superplastic deformation while the latter one represents DRX. During the initial stages of deformation, this alloy first dynamically recrystallizes and refines the grain size which is stabilized by the oxide particles in the matrix which prevent grain growth during high temperature deformation. Such stable fine grained structure promotes superplasticity during further

deformation if done at slow strain rates and higher temperatures. On the other hand, at higher strain rates and higher temperatures, DRX occurs. Thus, there is ample scope for designing suitable processes for making shapes in this material. In contrast, the gas atomized material does not exhibit any tendency for superplastic flow since the oxide particle content in the microstructure is not sufficient to prevent grain growth and to retain a stable fine grained structure during deformation.

The regime of flow instability, wherein the instability parameter $\xi(\dot{\varepsilon})$ is negative (Eq. 3), is marked by a thick line in the processing maps given in Figs. 3 and 4. From a comparison between the instability regimes in these two figures, it is clear that the gas atomized material is more prone to flow instability particularly at strain rates higher than 1.0 s^{-1} while the water atomized alloy is nearly free from instabilities at high strain rates. The manifestation of these instabilities has been found to be flow localization, which has to be avoided in the microstructure for achieving superior dynamic properties in the component.

(ii) Fe_3Al Alloys

The true stress – true strain curves obtained on binary Fe_3Al at a temperature of 1000°C and at different strain rates are shown in Fig.5.

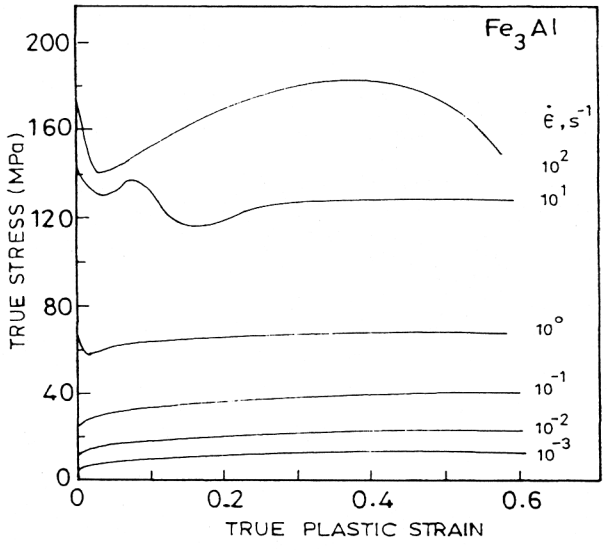

Fig. 5 True stress – true plastic strain curves obtained on binary Fe_3Al at a temperature of 1000°C and at different strain rates.

At strain rates below 0.1 s^{-1}, the material exhibits steady state behavior while at higher strain rates, initial yield drops, flow softening and oscillations are observed. The behavior of the Fe_3Al-Cr alloy is essentially similar to that described above. The flow stress values at different temperatures and strain rates are also not widely different. However, Fe_3Al-Mn alloy is much stronger than the above two and the true stress – true strain curves are of steady state type up to a strain rate of 1.0 s^{-1} (Fig.6). The stress – strain features alone do not lead to any definite conclusion on the deformation mechanisms.

On the basis of the kinetic rate equation (Eq.1) relating the flow stress to temperature and strain rate at a constant strain, apparent activation energy for hot deformation has been estimated using standard kinetic analysis. An apparent activation energy of about 260 kJ/mole has been estimated for the Fe_3Al alloy and this value matches well with that for the diffusion of Al in Fe_3Al [21]. On the other hand, much higher values have been estimated for the ternary alloys Fe_3Al-Cr (340 kJ/mole) and Fe_3Al-Mn (350 kJ/mole). To evaluate the mechanisms of hot deformation, these activation energy values are not very helpful although the higher values in the case of the ternary alloys are indicative of strengthening by the respective alloying elements. With a view to obtain optimum hot working conditions, processing maps have been developed and interpreted for these iron aluminide alloys.

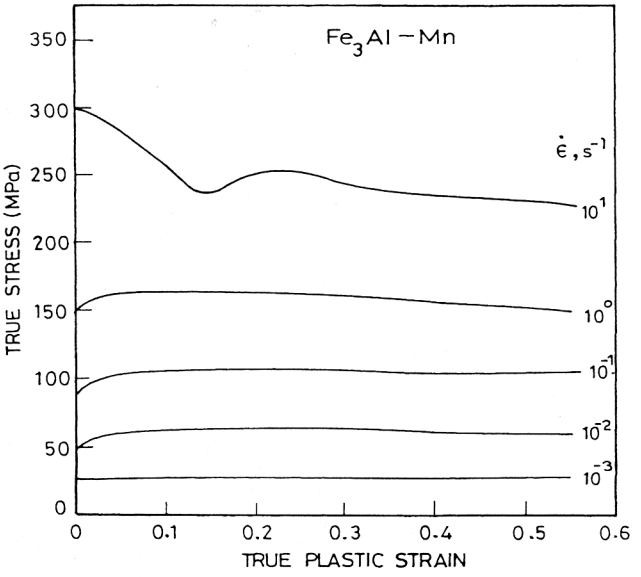

Fig. 6 True stress – true plastic strain curves obtained on ternary Fe_3Al-Mn material at a temperature of 950°C and at different strain rates.

The processing map for the binary Fe_3Al is shown in Fig. 7, which corresponds to a strain of 0.4. The maps at other strains are essentially similar. The map exhibits a single domain in the temperature range 850 – 1050°C and strain rate range 0.001 – 100 s^{-1} with a peak efficiency of 46% occurring at 1050°C and in the strain rate range 0.001 and 0.01 s^{-1}. Such a wide domain is indicative of excellent processability of the material. On the basis of detailed microstructural studies and grain size measurements on specimens deformed under conditions within this domain, it is interpreted [4] to represent DRX process. The processing map for Fe_3Al-Cr at a strain of 0.4 is shown in Fig. 8 and this also exhibits a single domain with a peak efficiency of 46% occurring at about 1000°C and at a strain rate of 0.001 s^{-1}.

The microstructural characteristics in this domain are similar to those in the binary alloy and hence the domain is interpreted [22] to represent DRX. However, this domain appears to have moved to lower temperatures and strain rates compared to the binary alloy. At higher temperatures (>1025°C), however, the peak efficiency has shifted to a higher stain rate, of about 0.1 s^{-1} due to dynamic grain growth. The processing map for Fe_3Al-Mn is shown in Fig.9, which also exhibits a single domain in the

temperature range 800 – 1050°C and at strain rates lower than 0.01 s^{-1} with a peak efficiency of about 59% occurring at 950°C/0.001 s^{-1}. The microstructure of the specimen deformed under conditions of peak efficiency has shown fine subgrains

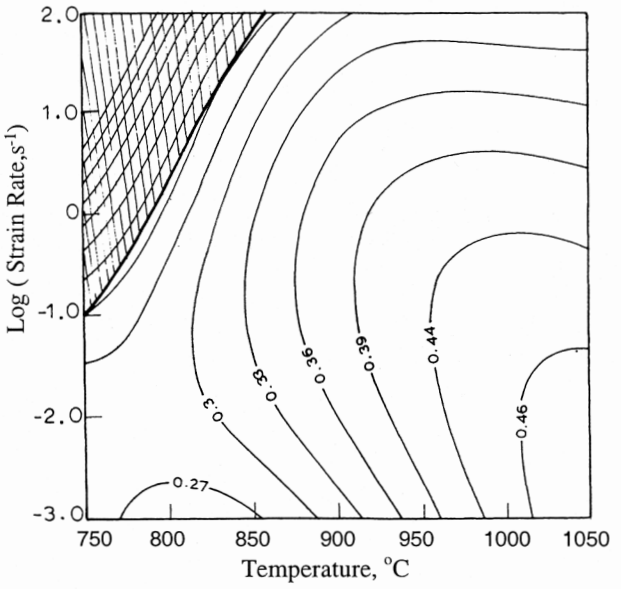

Fig. 7 Processing map for binary Fe_3Al obtained at a strain of 0.4. The numbers against each contour represent efficiency as a fraction. Flow instability is predicted to occur in the hatched regime.

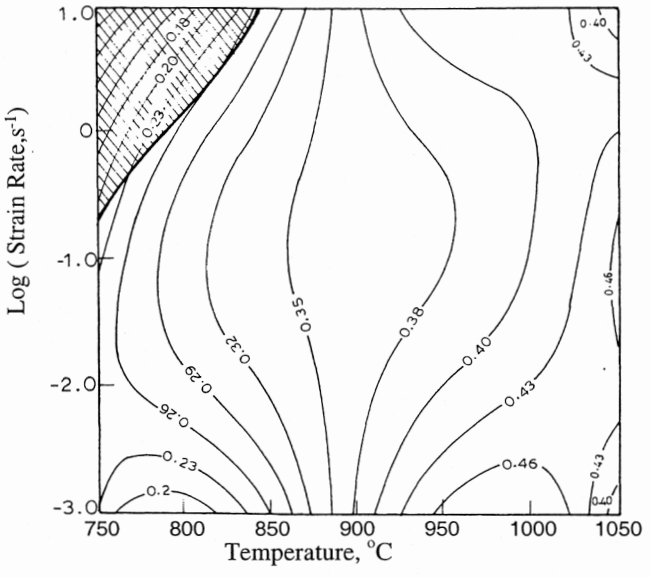

Fig. 8 Processing map for ternary Fe_3Al-Cr alloy obtained at a strain of 0.4. The numbers against each contour represent efficiency as a fraction. Flow instability is predicted to occur in the hatched regime.

basis of these observations, the domain is interpreted to represent large grained superplasticity (LGSP). Such a process requires a stable subgrain structure to be present in the microstructure and the presence of Mn may have slowed the rate of diffusion such that the grain boundary migration is somewhat restricted.

As regards the flow instability, the binary Fe_3Al and Fe_3Al-Cr alloys exhibit flow instabilities at temperatures lower than about 850°C and at strain rates above 0.1s^{-1}. These are in the form of flow localization. On the other hand, Fe_3Al-Mn did not exhibit any flow instability regime in the processing map.

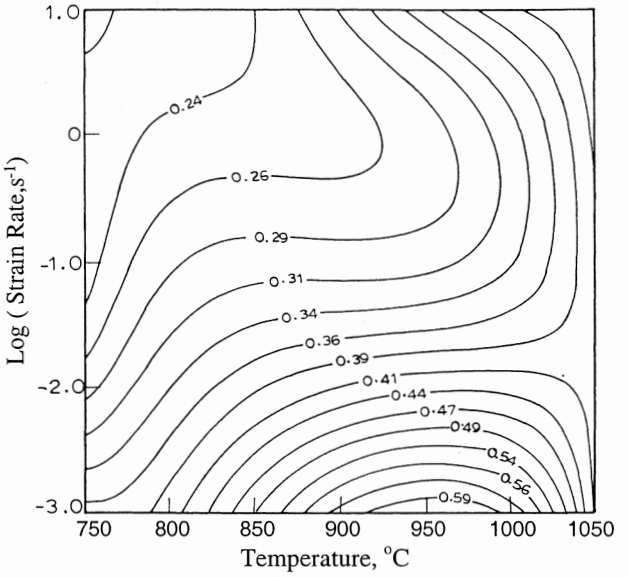

Fig. 9 Processing map for ternary Fe_3Al-Mn alloy obtained at a strain of 0.4. The numbers against each contour represent efficiency as a fraction.

The above results indicate that the addition of Mn to Fe_3Al is highly beneficial since it strengthens the material and makes it superplastic. Further, the material may be processed without the onset of flow instabilities. On the other hand, Cr additions do not have substantial influence on the processing behavior of Fe_3Al although they are beneficial in improving the room temperature ductility of the material [23].

Conclusions

1. The optimum hot working conditions for gas atomized FeAl alloy are 1100°C and 0.1 s^{-1}, which are the conditions for efficient DRX process.

2. The water atomized FeAl alloy may be superplastically formed at 1150°C and 0.001 s^{-1} since the fine oxide particles help in retaining the fine grained structure during deformation.

3. The water atomized FeAl may be processed at much faster speeds since it does not exhibit flow instabilities at higher strain rates while the gas atomized FeAl requires slower strain rates (<3 s^{-1}).

4. Fe_3Al based alloys have apparent activation energies lower than FeAl based alloys and require in general slower strain rate and lower temperatures for processing.

5. Mn containing Fe_3Al alloy exhibits large grain superplasticity and can be processed in a wide temperature window without the onset of flow instabilities.

6. Cr addition to Fe_3Al does not have significant influence on the hot workability or the mechanisms of hot deformation.

References

1. C.T.Liu, E.P.George, P.J.Maziasz and J.H.Schneibel, Mater. Sci. Eng. A258(1998)84.

2. N.S.Stoloff, Mater. Sci. Eng. A258(1998)1.

3. D.J.Alexander, P.J.Maziasz and J.L.Wright, Mater. Sci. Eng. A258(1998)276.

4. R.S.Sundar, R.G.Baligidad, Y.V.R.K.Prasad and D.H.Sastry, Mater. Sci. Eng. A258(1998)219.

5. M.R.Hajaligol, S.C.Deevi, V.K.Sikka and C.R.Scorey, Mater. Sci. Eng. A258(1998)249.

6. D.Lin, in: Nickel and Iron Aluminides – Processing, Properties and Applications, Eds. S.C.Deevi, V.K.Sikka, P.J.Maziasz, R.W.Cahn, Materials Park, Ohio: ASM International, 1997, p.187.

7. D.Lin and Y.Liu, Mater. Sci. Eng. A268(1999)83.

8. Y.V.R.K.Prasad and T.Seshacharyulu, Inter. Mater. Rev. 44(1998)243.

9. J.J.Jonas, C.M.Sellars, W.J.McG. Tegart, Metall. Rev. 14(1969)1.

10. Y.V.R.K.Prasad, H.L.Gegel, S.M.Doraivelu, J.C.Malas, J.T.Morgan, K.A.Lark, and D.R.Barker, Metall. Trans. A 15(1984)1883.

11. Y.V.R.K.Prasad and S.Sasidhara, Hot Working Guide: A Compendium of Processing Maps, Materials Park, Ohio: ASM International, 1997.

12. H.Ziegler, in: Progress in Solid Mechanics, Vol. 4, Eds. I.N.Sneddon and R.Hill, Amsterdam:North Holland Publishing Co., 1963, p.93.

13. Y.V.R.K.Prasad, D.H.Sastry and S.C.Deevi, Intermetallics 8(2000)1067.

14. J.D.Whittenberger, Mater. Sci. Eng. A57(1983)77.

15. J.D.Whittenberger, Mater. Sci. Eng. A77(1986)103.

16. U.Reimann and G.Sauthoff, Intermetallics 7(1999)427.

17. O.Tassa, C.Testani, B.Ricci Bitti, Scripta Metal. Mater. 26(1992)1913.

18. M.Eggersmann, B.Sepiol, G.Vogl, H.Mehrer, Defect Diffu. Forum 339(1997)143.

19. E.Kentzinger, M.S.Cadeville, V.Pierron-Bohnes, W.Petry, B.Hennion, J. Phys. Condens. Matter 8(1996)5535.

20. Y.V.R.K.Prasad, D.H.Sastry and S.C.Deevi, Mater. Sci. Eng. (in print)

21. L.K.Larikov, V.V.Geichenko and V.M.Falchenko, in Diffusion Process in Ordered Alloys, New Delhi: Oxionian, 1981,p.111.

22. R.S.Sundar, Processing and Creep Studies on Fe_3Al based Alloys, Ph.D. Thesis, Indian Institute of Science, Bangalore, India, 1998.

23. C.G.McKamey, J.A.Horton and C.T.Liu, J. Mater. Res. 4 (1989)1156.